



HAL
open science

Fabrication and characterization of copper and copper alloys reinforced with graphene

Antoine Bident, Florence Delange, Christine Labrugère-Sarroste, Catherine Debiemme-Chouvy, Yongfeng Lu, Jean-françois Silvain

► **To cite this version:**

Antoine Bident, Florence Delange, Christine Labrugère-Sarroste, Catherine Debiemme-Chouvy, Yongfeng Lu, et al.. Fabrication and characterization of copper and copper alloys reinforced with graphene. *Journal of Composite Materials*, 2024, 58 (1), pp.109-117. 10.1177/00219983231215210 . hal-04314387

HAL Id: hal-04314387

<https://hal.science/hal-04314387>

Submitted on 29 Nov 2023

HAL is a multi-disciplinary open access archive for the deposit and dissemination of scientific research documents, whether they are published or not. The documents may come from teaching and research institutions in France or abroad, or from public or private research centers.

L'archive ouverte pluridisciplinaire **HAL**, est destinée au dépôt et à la diffusion de documents scientifiques de niveau recherche, publiés ou non, émanant des établissements d'enseignement et de recherche français ou étrangers, des laboratoires publics ou privés.

Fabrication and characterization of copper and copper alloys reinforced with graphene

Antoine Bident^{1,2}, Florence Delange², Christine Labrugere³,
Catherine Debiemme-Chouvy⁴, Yongfeng Lu⁵ and
Jean-François Silvain^{1,5} 

Abstract

The consistent rise in current density within electrical wires leads to progressively more substantial heat losses attributed to the Joule effect. Consequently, mitigating the electrical resistivity of copper wires becomes imperative. To attain this objective, the development of a composite material that incorporates a more conductive reinforcement, like graphene, holds great promise. The conception of a copper/graphene composite using a powder metallurgy-based approach is presented. An optimum graphene quantity of 0.06 vol.% was obtained by calculation in order to limit the phenomenon of overlapping layers. This synthesis technique enables the dispersion of graphene and the meticulous control of the interface through the growth of CuO(Cu) nanoparticles that are tightly bonded to the reinforcement. The increase in the hardness of the various materials with separation of the graphene sheets by ultrasonic treatment (55.3 to 67.6 HV) was obtained. It is an indicator of the correct distribution of the reinforcement. The influence on the electrical properties of dendritic copper ($\rho_e = 2.30 \mu\Omega\cdot\text{cm}$) remains limited, resulting in a modest reduction in electrical resistance of around 1.4%. Nevertheless, for flake copper (2.71 $\mu\Omega\cdot\text{cm}$) and brass (7.66 $\mu\Omega\cdot\text{cm}$), we achieved a more substantial reduction of 2.7% and 10%, respectively. With the improvement of graphene quality, there exists a greater potential for further enhancing the electrical properties.

Keywords

graphene, surface treatment, hardness, electrical conductivity, composites, copper, powder metallurgy

Introduction

Currently, copper (Cu) is the most widely used metal for electrical systems. This is mainly due to its mechanical properties, particularly its ductility which allows for easy shaping; as well as its electrical resistivity, which is among the lowest among metals (1.78 $\mu\Omega\cdot\text{cm}$ at 20 °C¹). When a significant current density is applied to an electrical system, a non-negligible portion of energy is lost as heat. This phenomenon is known as Joule heating, and can result in energy losses (close to 10% according to I'IEA²) and potentially damage to the system if not properly managed. The use of a material with a lower electrical resistivity appears to be a viable solution to address this issue.

Only silver (Ag) can meet this criterion but the expensive costs exclude itself from industrial applications (8.8 €/kg for Cu against 750 €/kg for Ag³). An alternative is to develop a composite material using a reinforcement that is less resistive than Cu. From our knowledge, only graphene (Gr) can fulfil this requirement for an application involving 2D

materials. Known since the 1960s, it was only in 2004 that K. Novoselov and A. Geim⁴ were able, for the first time, to isolate graphene sheets using mechanical exfoliation, commonly called the “scotch trick”. The great attraction of scientists to this 2D material comes from the sp^2 hybridization of carbon atoms. In this case, two of the valence

¹Univ. Bordeaux, CNRS, Bordeaux INP, ICMCB, Pessac, France

²Schneider Electric SAS, Grenoble, France

³CNRS, Univ. Bordeaux, Pessac, France

⁴Sorbonne Université, CNRS, Laboratoire Interfaces et Systemes Electrochimiques, Paris, France

⁵Department of Electrical and Computer Engineering, University of Nebraska-Lincoln, Lincoln, USA

Corresponding author:

Jean-François Silvain, Department of Material Sciences, ICMCB-CNRS, 87 Avenue du docteur Albert Schweitzer, Pessac 33608, France.
Email: jean-francois.silvain@icmcb.cnrs.fr

Data Availability Statement included at the end of the article

orbitals P_x and P_y will form σ bonds in the plane of the graphene (which is the origin of the hexagonal structure). This allows a delocalization of the P_z orbital directed perpendicularly to the graphite plane. The overlapping of these P_z orbitals allows the formation of π - π^* bonds between carbon atoms, which are responsible for amazing electronic properties.^{5,6} As a result, Gr has a unique band structure with a semiconductor-like behaviour with a zero bandgap. This allows electrons to flow through the structure without collision, thus adopt a ballistic behaviour. These characteristics of Gr lead to exceptional electrical properties (200,000 cm^2/vs , again 33 cm^2/vs for Cu⁷), thermal properties (5600 W/mK,⁸ compare to 400 W/mK for Cu), and mechanical properties (Young's modulus of 1 TPa and tensile strength of 130 GPa⁹). Due to these properties, the Gr has been used as a reinforcement in various types of composite materials such as polymers, metals, or ceramics. However, the different methods to fabricate these composites have their own advantages and disadvantages that affect the final properties. Nevertheless, based on powder metallurgy (used in this study), three main points are important to master in order to obtain a high-performance composite material.

The first two factors to be considered are the distribution¹⁰ and orientation of the Gr reinforcement within the matrix.¹¹ An agglomeration of several graphene layers or a significant overall misorientation of the reinforcement will result in the degradation of the macroscopic properties of the composite materials. The reinforcement-matrix (R-M) interface is also critical for ensuring proper transfer of properties between both materials. However, Cu and carbon have no chemical affinities leading to a poor interfacial property transfer. Two methods exist to create interfacial chemical bonding: the first involves using a carbide element which will react with carbon to form carbide interphase.¹² However, the formation of this carbide interphase is associated with the reaction of carbon and therefore of the degradation and/or the total of consumption of Gr, making this method inappropriate for nanometric carbon-based reinforcement. The second method involves the growth of metallic nanoparticle, chemically linked with the carbon atom surface of Gr, on the surface of the reinforcement.¹³ These particles can be made from various materials (Cu, Ag, Cr, Ni^{14,15}). Cu will be chosen to match the matrix. Nevertheless, there are very few articles reporting a decrease in electrical resistivity of such a composite compared to pure Cu. Keerti S. et al.¹⁶ show a 2.7% increase in electrical conductivity of pure Cu with the incorporation of 15 ppm (0.006 vol.%) of graphene, while Mu Cao's team¹⁷ obtained over 15% increases in electrical conductivity compared to pure Cu. However, the fabrication method employed by the latter is too sophisticated to be viable for industrial applications. However, these two studies remain exceptions because in most cases (i.e.,^{18,19}) increases in electrical

resistivity are obtained following the preparation of graphene reinforcement composites.

In this work, Cu/Gr and brass/Gr composite materials were fabricated using conventional powder metallurgy processes. A first surface treatment of the Gr involves an acid treatment to remove surface contamination and graft oxygen functional groups. Then, a second treatment enables the growth of Cu nanoparticles (on the functionalized groups) that will be chemically bonded to the Gr. Subsequently, an innovative method for mixing copper powder and graphene will be used to obtain a homogeneous powder without degradation. Finally, the powders will be densified using a hot uniaxial pressing method. Hardness and electrical conductivity were measured on each sample and compared to non-reinforced materials. The main goal was the increase of the electrical conductivity of the composite (positive composite effect), which is a novel and rarely represented work in the literature.

Materials and methods

Raw materials

Dendritic Cu (Cu-D) powder with an average length size of 50 μm and a diameter of 10 μm , and flake Cu (Cu-P) powder with an average width of 20 μm and a thickness of 350 nm were purchased from ECKART (Figure 1(a) and (b)). Flake brass (Bra-P) (80% Cu, 20% Zn) powder, purchased from Werth-Metal, has an average length size of 40 μm and a diameter of 10 μm (Figure 1(c)). These powders were used as received without further treatment. Multilayer Gr powder (KNG-5) with a lateral size of 5–10 μm and an average thickness of 2–3 nm (3–9 atomic layers) were bought from KNANO Company. This MLG was made by a chemical exfoliation method of graphite.

Fabrication of the composite materials. First, homogenization of the Gr reinforcement in an ethanol solution of 0.1 g/L concentration was carried out using an acoustic mixer, with an acceleration of 80 g for 6 min. An acoustic type mixer (LABRAM II Resodyn) was then used in order to reach an optimal "matrix + reinforcement". In this process, the "ethanol + Gr solution" was spread on the surface of the Cu powders which were in levitation induced by the acoustic wave of the mixer. In order to reduce the surface oxidation of the Cu powder as well as the CuO nanoparticles, the composite powder "Cu + Gr" obtained was dried and reduced in a furnace at 400 °C for 60 min under a flow of Ar/5% H_2 . The densification of the composite materials was carried out using a Thermolab press equipped with an inductive heating system. The densification parameters are a temperature of 650 °C applied for 45 min under a pressure of 60 MPa in an inert atmosphere. Relative densities, equal or greater than 99% whatever the

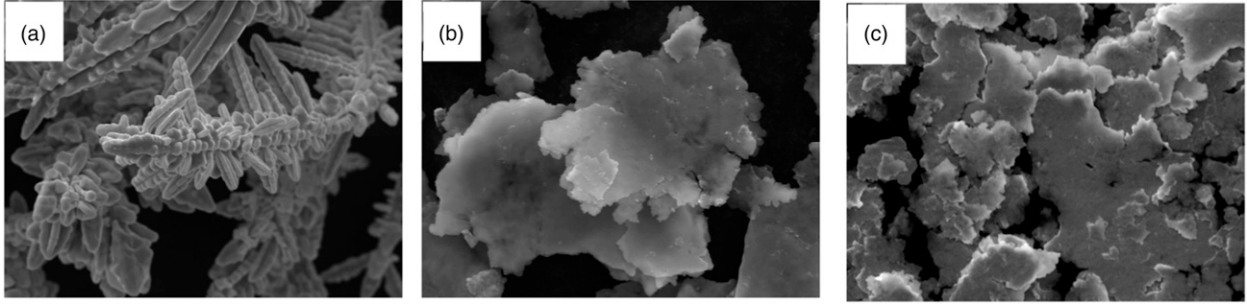


Figure 1. SEM analysis of dendritic and flake Cu (a) and (b) and flake brass (c).

materials, were measured using the Archimedes' displacement method.

Characterization method. Hardness of different materials was measured using the Micro-Vickers hardness method equipped with a square-based diamond pyramid tip. The measurements are performed in the plane perpendicular to the densification direction, using a force of 20 kgf to obtain the largest possible indentation. Each sample is indented ten times on both sides to ensure the lowest possible uncertainty. The electrical resistivity of the composites was measured by typical a four-point contact probe. Both outer tips are connected to the generator for current injection with an ammeter for current measurement. Both inner tips are connected to a nano-voltmeter for voltage measurement. This system was placed in a temperature-controlled oven to perform measurements at various temperatures. A thermocouple was also placed under the sample to obtain an accurate temperature value. A copper alloy sample ($\rho_{e\ 20^\circ\text{C}} = 1.724\ \mu\Omega\cdot\text{cm}$, and a purity of 99.9 wt.% in copper) was purchased to ensure that the measurements of our 4-point system are correct.

Cu nanometric particles were characterized by transmission electron microscopy (TEM) using a JEOL-2100 microscope. Analysis of the Gr surface was carried out using a ThermoFischer Scientific K-Alpha® X-ray photoelectron spectrometer system with a monochromatized Al K α source ($h\nu = 1486.6\ \text{eV}$) and a spot size of 200 μm . Full and high-resolution spectra obtained were fitted using the AVANTAGE software provided by ThermoFischer Scientific®. Scofield sensitivity factors were used for quantification. The measurements were conducted with a precision of $0.1\ \text{cm}^{-1}$ using a high-resolution Jobin Yvon Horiba LabRam HR micro-Raman spectrometer equipped with a charge coupled device (CCD) detector. Raman spectra were obtained in scattering micro-configuration. The incident laser light as well as the backscattered light are focused by a $10\times$ objective.

Results and discussion

Determination of the optimal amount of Gr reinforcement

To determine the percolation threshold value for an “ideal” material, where half of the metallic powders are covered by one Gr sheet, the calculation of the required Gr content is proposed. The aim is to avoid the contact between two Gr particles during the assembly of the Cu powder, which would result in the presence of nano-porosity I between 2 Gr sheets which is assumed to be harmful for the electrical properties.

The geometry of the KNG-5 Gr and Cu-P powder are taken into account in these calculations. First, the equation (1) allows to calculate the surface areas of Cu and Gr particles.

$$S_{Cu} = \frac{(1 - \%wt)}{V_{Cu} \times \rho_{Cu}}; S_{Gr} = \frac{\%wt}{V_{Gr} \times \rho_{Gr}}, \quad (1)$$

where S_{Cu} and S_{Gr} are the surface areas of Cu and Gr in cm^2 , wt.% is the weight percentage of the reinforcement, ρ_{Cu} and ρ_{Gr} are the density of Cu ($8.9\ \text{g/cm}^3$) and graphene ($2.2\ \text{g/cm}^3$), respectively, and V_{Cu} and V_{Gr} are the volumes of Cu and graphene particles in cm^3 .

To determine the coverage percentage of Cu by Gr particles, we need to calculate the ratio of the surface areas of the Gr particles to those of the Cu particles. This can be done using the following equation (2), with its representation in Figure 2.

$$S_{Gr}/S_{Cu} = \frac{\frac{\%wt}{V_{Gr} \times \rho_{Gr}}}{\frac{(1-\%wt)}{V_{Cu} \times \rho_{Cu}}} = \frac{\%wt \times V_{Cu} \times \rho_{Cu}}{(1 - \%wt) \times V_{Gr} \times \rho_{Gr}}. \quad (2)$$

According to this graph, a quantity of 0.06 vol.% of graphene seems sufficient to cover half of the surface areas of the Cu-P powders. In the case of our materials, a quantity of graphene corresponding to an initial content of 0.1 vol.% were

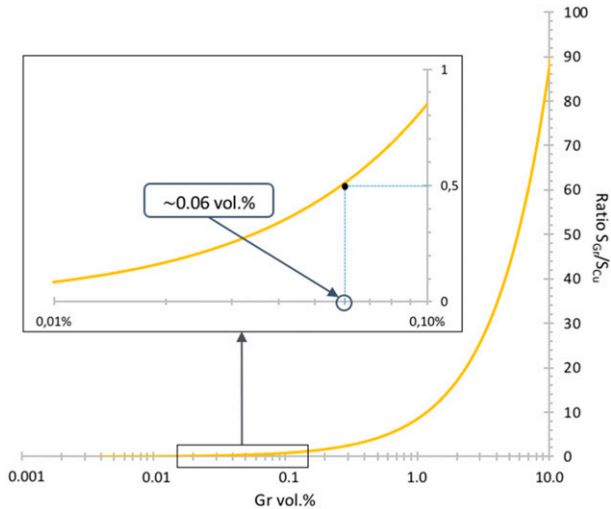


Figure 2. Evolution of the S_{Gr}/S_{Cu} ratio as a function of the percentage of Gr inside the composite materials.

used to compensate for losses induced by the various steps. The same Gr amount were used for both dendritic Cu and brass flakes. Obviously, this is a numerical calculation in an ideal case, and it is impossible to achieve such a model. Nevertheless, it allows us to obtain an approximate value for the quantity of Gr required to reach the percolation threshold without inducing overlapping.

The calculated Gr content may seem low compared to the majority of the recent works in the literature,²⁰ where graphene contents higher than 1 vol.% were used. However, as seen in various works,²¹ percolation thresholds around 0.1 vol.% are often obtained.

Studying the impact of the graphene quantity (beyond the percolation threshold) on the electrical properties of the composite material would be interesting. However, this aspect will be addressed in a separate publication.

As mentioned previously, Cu and Gr are two materials chemically inert. Therefore, a preparation step of the Gr reinforcement, including chemical treatment of Gr and germination-growth of nanometric Cu particles onto Gr surface, is necessary.

Surface treatment and functionalization of the graphene materials

To disperse the Gr materials, acoustic mixing (80 g for 10 min) has been applied on alcohol + Gr mixture. After this first treatment, nitric acid (HN) treatment has been used to modify the surface chemistry of the Gr powder. Specific conditions of the mixing and acid treatment can be found in.²² A treatment time ranging from 0 to 150 min was applied at a temperature of 100 °C in a reflux setup equipped with a water-cooled condenser and magnetic stirring. XPS analysis has been performed to characterize

Table 1. Evolution of the O and C percentages: XPS analysis of the HN treated and non-treated Gr materials.

Treatment time (min)	C (%)	O (%)
0	98.5	1.5
30	98.5	1.5
150	98.5	1.5

the evolution of the surface chemistry of the non-treated and treated Gr powders. Table 1 shows the evolution of the carbon (C1s) and oxygen (O1s) atomic percentages with the treatment time. No specific effect can be observed. After deconvolution, the C1s spectra is presented in the Figure 3; the association of the different contributions with their binding energy was obtained from these following articles R. Al-Gaashani and D. Ferrah et al.^{23,24} Table 2 shows the evolution of the Csp² and π - π^* percentage (corresponding to the contribution of carbon sp² hybridization and π - π^* bonding) and the Csp²/Csp³ ratio. In the two-dimensional structure of Gr, each carbon atom is strongly bonded to three neighbors (σ bonds) with an angle of 120° in the plane. This structure is the consequence of the sp² hybridization of the carbon atoms and the sp³ hybridization is related to the disorder or amorphous carbon. This configuration allows the non-hybridization (delocalization) of the carbon pz orbital which is found directed perpendicular to the graphitic plane. It is the overlapping of these orbitals that allows the formation of the π - π^* bonds that are the origin of the astonishing electronic properties of Gr.⁵

Table 1 shows that the HN treatment has no effect on the evolution of the chemistry of the Gr surface (C and O are constant, independent of the treatment time). After deconvolution of the high-resolution C1s peak, table 2 shows that the concentration of the Csp² species increases with the treatment time. It seems unlikely that this increase is attributable to a “restoration” of the graphitic network. It is more likely that the acid treatment leads to the elimination of surface contamination from the Gr materials.

However, with regard to the evolution of the percentage of the π - π^* bonds, the material seems to undergo a slight degradation (cf. Table 2). Therefore, a short treatment time is preferable to limit deterioration and eliminate some of the contamination. A time of 30 min was therefore selected.

To enable the germination growth of copper nanoparticles on the entire surface of the reinforcement, a dispersion step of the graphene in the solution (ethanol) is necessary. To achieve this, ultrasonic agitation for a time ranging from 10 s to 90 min was performed. To monitor the evolution of the separation of the graphene layers, an analysis by UV-Visible spectroscopy was performed (cf. Figure 4). In our case, since the graphene serves as a density filter, an increase in the absorbance of the solution would

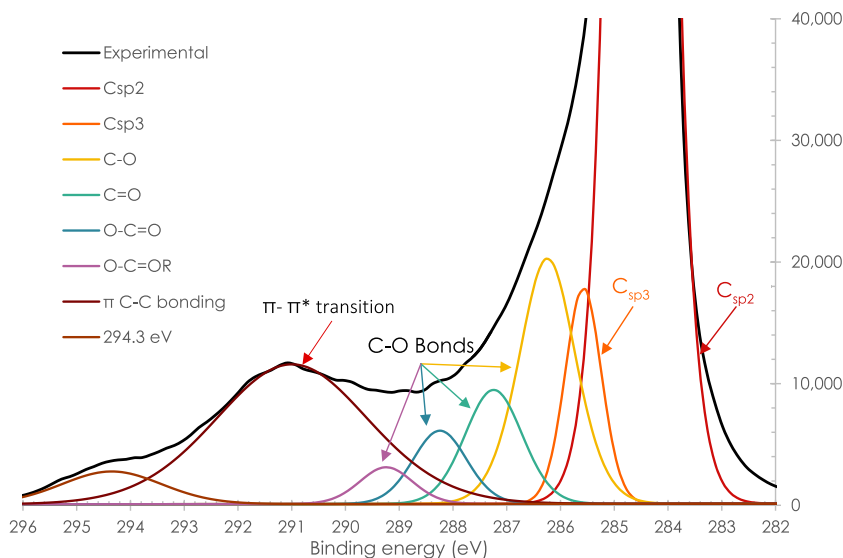


Figure 3. Deconvolution of a high-resolution C1s peak of MLG.

Table 2. Evolution of the CIs contributions with different HN treatment time.

Treatment time (min)	Csp2 (%)	C_{sp2}/C_{sp3}	$\pi - \pi^*$ (%)
0	69.0	10.3	9.3
30	70.5	13.4	8.6
150	73.0	15.1	7.6

indicate an increase in the amount of layers present, i.e., exfoliation of the graphene layers.

As can be seen, an increase in the ultrasonic treatment time leads to an increase in the absorbance of the solution. This graph also shows that the separation of the layers reaches its maximum after a 5 min treatment, with the absorbance of the solution remaining constant up to an hour of treatment. Raman analyses, allowing the calculation of the I_D/I_{2D} ratio (used instead of the I_D/I_G ratio for higher sensitivity²⁵), show that during this first hour, the reinforcement is not degraded by the ultrasonic treatment (Table 3). On the contrary, a decrease in the Raman ratio is obtained.

It was also observed that the absorbance increases again after 60 min, indicating an increase in the number of graphene layers. However, considering the evolution of the I_D/I_{2D} ratio, obtained by Raman spectroscopy (cf. Table 3), this new increase in the absorbance is accompanied by an increase in the I_D/I_{2D} ratio, indicating that we no longer have a simple separation of the layers, but rather a rupture of the C-C bonds. A treatment time of 5 min appears to be optimal.

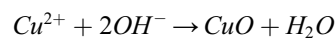
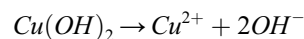
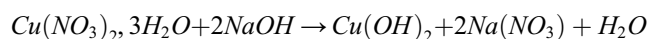
After this optimized HN treatment, CuO (Cu after Ar/5% H₂ treatment) nanoparticles were grown of the surface of the

Gr materials treated²². For that, two solutions are prepared initially:

- Solution 1: 0.5 g of sodium hydroxide (NaOH) in 25 mL of water.
- Solution 2: 1 g of hydrated Cu nitrate (Cu(NO₃)₂, 3H₂O) in 100 mL of ethanol.

Solution 1 and 2 are added dropwise under magnetic stirring, and then placed in a reflux setup at 90 °C. These initial steps aim to promote the nucleation of Cu hydroxide in a basic medium, followed by the formation of Cu (II) oxide.

Associated reactions:



The CuO particles are then thermally reduced at 400 °C for 1 h under a reducing atmosphere (Ar/5%H₂).

Transmission electron microscopy (TEM) analysis shows that for the optimized growth and reduction heat treatment in a Ar/5% H₂ atmosphere, Cu particles with a mean diameter of 16.8 ± 7.1 nm are grown of the Gr surfaces (cf. Figure 5). The micro diffraction pattern of one Cu dot shows that the nanodots are perfectly crystallize (cubic face center of Cu).

To verify the presence of a strong chemical bond between the Cu nanoparticles and the surface of the reinforcement, an adhesion test was performed. The graphene solution was placed under an ultrasonic probe for 10 s. As

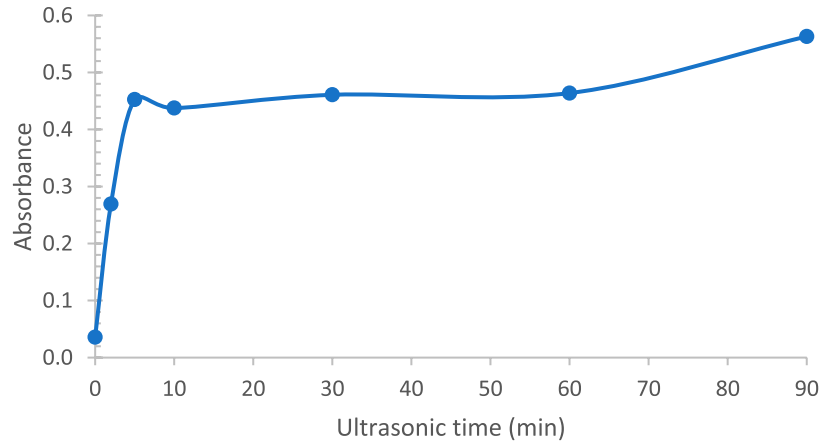


Figure 4. Evolution of the absorbance of different Gr solutions after various ultrasonic treatment times.

Table 3. Evolution of Raman ratio after several ultrasonic time.

Ultrasonic time (min)	I_D/I_{2D}
0	0.55
5	0.40
10	0.39
30	0.45
60	0.46
90	0.93

shown in Figure 6(c), the Cu nanoparticles (white dots on the Gr surfaces) are still present on the surface of the reinforcement, although the particle density is slightly lower than the initial one (cf. Figure 6(a)). Another reinforcement was tested without a surface contamination removal pretreatment (cf. Figure 6(b)). The Cu nanoparticles were removed by the ultrasonic treatment due to the formation of bonds with the contamination present on the surface of the graphene, weakly bound to the reinforcement. Therefore, it is essential to eliminate this surface contamination.

Characterization of dense material

Hardness. The material hardness was measured to highlight the impact of the reinforcement (cf. Table 4). As a reminder, an ultrasonic finger device and a germination method were used to individualize the graphene sheets to the maximum extent and optimize the electrical and mechanical properties of the material. Initially, it was observed that the simple introduction of the reinforcement (without graphene sheet individualisation treatment) does not induce a significant increase in the hardness of the different copper and copper alloys studied, due to the low amount of reinforcement present (0.06 vol.%) and graphene agglomeration. Secondly, it is noticed that carrying out an ultrasonic treatment induces a significant increase in material hardness, i.e., with

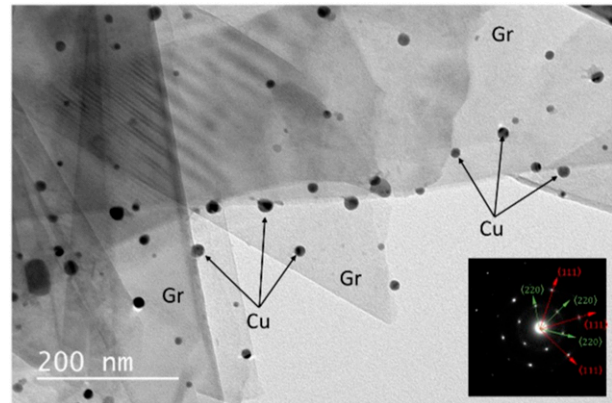


Figure 5. TEM micrograph and micro diffraction pattern of the Cu nanoparticles (black dots on the Gr surfaces) grown on the surface of treated HN Gr surfaces.

an increase of about 12 HV for Cu-D/Gr. This result remains consistent because the reinforcements are a resistance to material deformation and the movement of dislocations. Therefore, the more particles present (induced by separating the sheets using ultrasonic treatment), the more the material hardness would increase. The evolution of material hardness is thus a relevant indicator to attest to the homogeneous distribution of reinforcement in the material, thereby optimizing the mechanical properties of the composite materials.

Electrical resistivity. The electrical resistivity measurements were carried out on our materials. The results are shown in Figure 7. Concerning the Cu-D/Gr composite, it can be observed that the decrease in electrical resistivity is only 1.4% compared to Cu-D without reinforcement. The error range in the measurement has been estimated to be approximately 1%, so this value remains relevant. The introduction of Gr therefore has a relatively small impact on

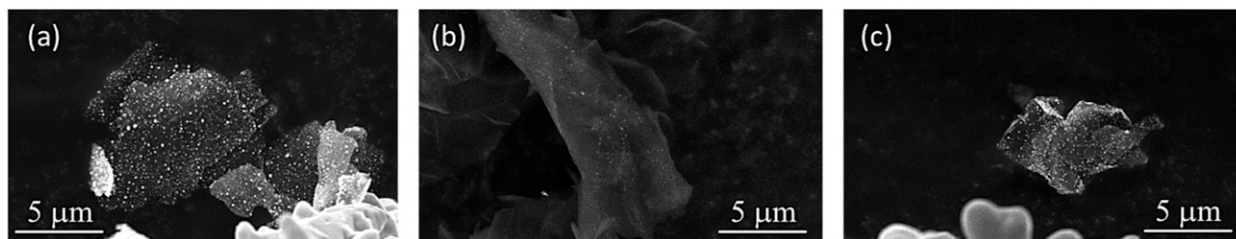


Figure 6. SEM micrograph of an (a.) graphene sheet with Cu(O) nanoparticles without HN pre-treatment, (b.) graphene sheet with Cu(O) nanoparticles without HN pre-treatment and after 10 s of ultrasonic treatment, (c.) graphene sheet with Cu(O) nanoparticles with HN pre-treatment and after 10 s of ultrasonic treatment.

Table 4. Evolution of the hardness of different composite materials.

Materials	Hardness with/without ultrasonic treatment of the Gr (HV \pm 1.2)	
	With	Without
Cu-D	55.8	
Cu-D/Gr	55.3	67.6
Cu-P	61.1	
Cu-P/Gr	61.5	72.4
Brass	120.2	
Brass/Gr	121.0	134.1

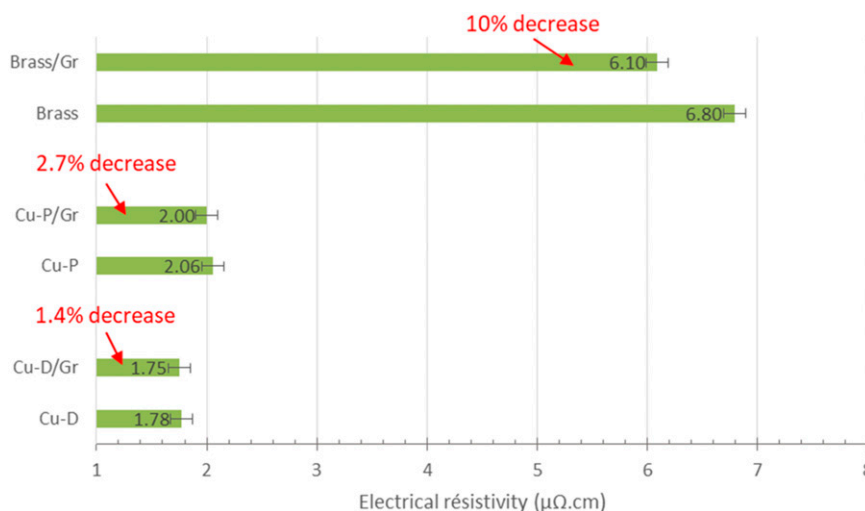


Figure 7. Electrical resistivity measurement at 20°C for various single and composite copper matrix materials.

the electrical resistivity, this is due to the very low electrical resistivity of Cu-D. Regarding Cu-P, which has higher electrical resistivity than Cu-D (2.06 against 1.78 $\mu\Omega.cm$), the decrease in electrical resistivity (for the Cu-P/Gr composite) is more significant, with a gain of 2.7%. The reason for this greater decrease could be due to a more favourable alignment of the Gr layers in a plane perpendicular to the pressing direction. However, measurements

carried out by polarized Raman spectroscopy (not presented in this study) disagree with this hypothesis. Consequently, the greatest decrease in electrical conductivity could be induced by the weaker initial electrical properties of the Cu used (Cu-P).

To validate this hypothesis, a final series of materials were produced using brass (Cu alloy with 20 wt.% of zinc) as the matrix; brass has a higher electrical resistivity

(6.8 $\mu\Omega\cdot\text{cm}$) than that of copper (1.78 $\mu\Omega\cdot\text{cm}$). The results of the electrical resistivity measurement show that the incorporation of graphene leads to a reduction in electrical resistivity to 6.1 $\mu\Omega\cdot\text{cm}$ (around 10%). In the case of this sample, we can see that the composite effect is present. Our hypothesis is therefore valid. The difference in electrical resistivity between the reinforcement and the matrix is not significant enough in the case of Cu-D. However, in the case of brass, the intrinsic resistivity of the matrix being lower, the composite effect is more significant.

Conclusions

In this study, a new method for developing Cu/Gr composites was developed, with significant focus on creating a high-performing interface through the germination growth of the CuO nanoparticles. Hardness measurements showed the importance of separating Gr layers to obtain a homogeneous distribution, resulting in increased material hardness. Results from electrical resistivity measurements indicated that using a matrix with higher resistivity than Cu leads to a greater positive composite effect. This validates our hypothesis and highlights that the intrinsic properties of Gr used are not sufficient for achieving a significant positive composite effect on Cu-D. This finding suggests the possibility of incorporating graphene into lower quality Cu or Cu alloys to increase their electrical conductivity and reduce the amount of Cu used, especially considering the shortage of Cu resources expected to occur within the next 50 years. Indeed, this approach would allow industries to use lower-quality Cu while achieving electrical properties very close to pure Cu through the development of a composite material. Furthermore, incorporating graphene reinforcement into materials with higher electrical resistivity, such as ferrous or Al alloys, may be feasible, although optimizing the R-M interfaces using an appropriate metallic salt will be necessary.

Author contributions

The work was completed through contributions of all authors. All authors have given approval to the final version of the manuscript. The individual contributions are: Supervision and conceptualization: Jean-François SILVAIN, Nathalie CAILLAULT, Florence DELANGE, Antoine BIDENT; Roles/Writing -original draft; and Writing - review & editing: Jean-François SILVAIN, Catherine DEBIEMME-CHOUVY, Yongfeng LU, Antoine BIDENT; Investigation: Antoine BIDENT.

Declaration of conflicting interests

The author(s) declared no potential conflicts of interest with respect to the research, authorship, and/or publication of this article.

Funding

The author(s) disclosed receipt of the following financial support for the research, authorship, and/or publication of this article: This study was supported by Schneider Electric SAS.

ORCID iD

Jean-Francois Silvain  <https://orcid.org/0000-0002-5881-6833>

Data availability statement

All data needed to support the conclusions in the paper and the datasets generated during the current study are available from the corresponding author on reasonable requests. Although strongly involved in open science (article and data; CNRS recommendations), we decided that the data from our article would be provided upon request.

References

1. Les propriétés du cuivre et de ses alliages, centre d'information du cuivre laitons et alliages, 1992. Variances – Edition.
2. IEA. Electricity information: overview, Paris. <https://www.iea.org/reports/electricity-information-overview> License: CC BY 4.0, 2021).
3. Boursorama. <https://www.boursorama.com/bourse/matieres-premieres/cours/7xCAUSD> (2023).
4. Novoselov KS, Geim AK, Morozov SV, et al. Electric field effect in atomically thin carbon films. *Science* 2004; 306(5696): 666–669. DOI: [10.1126/science.1102896](https://doi.org/10.1126/science.1102896).
5. Neto AHC, Guinea F, Peres NMR, et al. The electronic properties of graphene. *Rev Mod Phys* 2009; 81: 109. DOI: [10.1103/RevModPhys.81.109](https://doi.org/10.1103/RevModPhys.81.109).
6. Wallace PR. The band theory of graphite. *Phys Rev* 1947; 71: 622. DOI: [10.1103/PhysRev.71.622](https://doi.org/10.1103/PhysRev.71.622).
7. Bolotin KI, Sikes KJ, Jiang Z, et al. Ultrahigh electron mobility in suspended graphene. *Solid State Commun* 2008; 146(9): 351–355. DOI: [10.1016/j.ssc.2008.02.024](https://doi.org/10.1016/j.ssc.2008.02.024).
8. Kohyakov PA, Giovannetti G, Rusu PC, et al. First-Principle study of the interaction and charge transfer between graphene and metals. *Phys Rev B* 2009; 79: 195425. DOI: [10.1103/PhysRevB.79.195425](https://doi.org/10.1103/PhysRevB.79.195425).
9. Lee C, Wei X, Kysar JW, et al. Measurement of the elastic properties and intrinsic strength of monolayer graphene. *Science* 2008; 321(5887): 385–388. DOI: [10.1126/science.1157996](https://doi.org/10.1126/science.1157996).
10. Nirmalraj PN, Lutz T, Kumar S, et al. Nanoscale mapping of electrical resistivity and connectivity in graphene strips and networks. *Nano Lett* 2011; 11(1): 16–22. DOI: [10.1021/nl101469d](https://doi.org/10.1021/nl101469d).
11. Li W, Liu Y and Wu G. Preparation of graphite flakes/Al with preferred orientation and high thermal conductivity by squeeze casting. *Carbon* 2015; 95: 545–551. DOI: [10.1016/j.carbon.2015.08.063](https://doi.org/10.1016/j.carbon.2015.08.063).

12. Azina A. *Diamond-based multimaterials for thermal management applications*. PhD thesis. France: University of Bordeaux, 2017.
13. Giovannetti G, Khomyakov PA, Brocks G, et al. Doping graphene with metal contacts. *Phys Rev Lett* 2008; 101: 026803. DOI: [10.1103/PhysRevLett.101.026803](https://doi.org/10.1103/PhysRevLett.101.026803).
14. Li M, Che H, Liu X, et al. Highly enhanced mechanical properties in Cu matrix composites reinforced with graphene decorated metallic nanoparticles. *J Mater Sci* 2014; 49(10). DOI: [10.1007/s10853-014-8082-x](https://doi.org/10.1007/s10853-014-8082-x).
15. Luo H, Sui Y, Qi, et al. Copper matrix composites enhanced by silver/reduced graphene oxide hybrids. *Mater Lett* 2017; 186: 354–357. DOI: [10.1016/j.matlet.2017.03.084](https://doi.org/10.1016/j.matlet.2017.03.084).
16. Kappagantula KS, Smith JA, Nittala A, et al. Macro copper-graphene composites with enhanced electrical conductivity. *J Alloys Compd* 2001; 894: 162477. DOI: [10.1016/j.jallcom.2021.162477](https://doi.org/10.1016/j.jallcom.2021.162477).
17. Cao M, Xiong DB, Yang L, et al. Ultrahigh electrical conductivity of graphene embedded in metals. *Adv Funct Mater* 2019; 29(17): 1806792. DOI: [10.1002/adfm.201806792](https://doi.org/10.1002/adfm.201806792).
18. Ayyappadas C, Muthuchamy A, Raja Annamalai A, et al. An investigation on the effect of sintering mode on various properties of copper-graphene metal matrix composite. *Adv Powder Technol* 2017; 28(7): 1760–1768. DOI: [10.1016/j.apt.2017.04.013](https://doi.org/10.1016/j.apt.2017.04.013).
19. Dong LL, Chen W, Zheng C, et al. Microstructure and properties characterization of tungsten-copper composite materials doped with graphene. *J Alloys Compd* 2016; 695. DOI: [10.1016/j.jallcom.2016.10.310](https://doi.org/10.1016/j.jallcom.2016.10.310).
20. Fluke M, Kleinrahm R and Wagner W. Measurement and correlation of the (p, r, T) relation of nitrogen II. Saturated-liquid and saturated-vapour densities and vapour pressures along the entire coexistence curve. *J Chem Therm* 2002; 34(12): 2017–2039. DOI: [10.1016/S0021-9614\(02\)00266-5](https://doi.org/10.1016/S0021-9614(02)00266-5).
21. Alemour B, Myaacob MH and Hassan MR. Review of electrical properties of graphene conductive composites. *Int J Nanoelectro Mater* 2018; 11(4): 371–398.
22. Bident A. *Elaboration de matériaux composites cuivre/graphene à propriétés physiques améliorées par métallurgie des poudres*. PhD thesis. France: University of Bordeaux, 2022.
23. Al-Gaashani R, Najjar A, Zakaria Y, et al. XPS and structural studies of high quality graphene oxide and reduced graphene oxide prepared by different chemical oxidation methods. *Ceram Int.* 2019; 45(11): 14439–14448. doi:[10.1016/j.ceramint.2019.04.165](https://doi.org/10.1016/j.ceramint.2019.04.165)
24. Ferrah D, Rewnault O, Petit-Etienne C, et al. XPS investigations of graphene surface cleaning using H₂- and Cl₂-based inductively coupled plasma. *Surf Interface Anal* 2016; 48(7).
25. Cançado LJ, Jorion A, Martins Ferreira EH, et al. Quantifying defects in graphene via Raman spectroscopy at different excitation energies. *Nano Lett* 2011; 11(8): 3190–3196. DOI: [10.1021/nl201432g](https://doi.org/10.1021/nl201432g).